

# NAVIGATION PERFORMANCE ANALYSIS AND TRADES FOR THE LUNAR GNSS RECEIVER EXPERIMENT (LUGRE)

Lauren Konitzer,<sup>\*</sup> Nathan Esantsi,<sup>†</sup> and Joel Parker<sup>‡</sup>

The Lunar GNSS Receiver Experiment (LuGRE) is a joint NASA-Italian Space Agency flight demonstration payload that will fly onboard the Firefly Blue Ghost Mission 1 (BGM1) lunar lander to demonstrate multi-GNSS based position, navigation, and timing (PNT) in cislunar space and at the Moon. The LuGRE mission aims to receive GPS and Galileo signals at the Moon to characterize the lunar GNSS signal environment, demonstrate navigation and time estimation, and utilize collected data to support development of GNSS receivers specific to lunar use. Several key factors of the LuGRE design and concept of operations impact how navigation performance may be achieved during the mission, including available observables, limited measurement duration, limited data rates, and use of a lower-quality oscillator. This paper investigates the impacts of these factors and how they may inform the mission design and maximize science return.

## INTRODUCTION

The Lunar GNSS Receiver Experiment (LuGRE) is a joint NASA-Italian Space Agency flight demonstration payload that will fly onboard the Firefly Blue Ghost Mission 1 (BGM1) lunar lander with the goal of demonstrating multi-GNSS based position, navigation, and timing (PNT) in cislunar space and at the Moon.<sup>1</sup> The LuGRE payload will collect, process, and downlink GPS and Galileo signals in transit from the Earth to the Moon, in lunar orbit, and on the lunar surface. Signals acquired by LuGRE will be amongst the highest-altitude demonstrations of GNSS signals received to-date, achieving the critical milestone of multi-GNSS signals reception on the Moon. The data collected by LuGRE will open the door for future operational use of GNSS for lunar-vicinity PNT.

The 3<sup>rd</sup> edition of the International Space Exploration Coordination Group's Global Exploration Roadmap anticipates dozens of missions to the Moon within the coming decade, identifying navigation technology as a major enabler in support of lunar landing.<sup>2</sup> In a similar vein, NASA's 2020 Artemis Plan specifically names GPS-based navigation as a means for meeting the unique needs of lunar users.<sup>3</sup> GNSS is deliberately highlighted because while future lunar missions will surely utilize a broader multi-faceted lunar-based navigation framework<sup>4,5</sup>, users can already obtain precise PNT services with relatively low burden to size, weight, power, and cost (SWaP-C) by leveraging

---

<sup>\*</sup> Aerospace Engineer, Navigation and Mission Design Branch. NASA Goddard Space Flight Center, Greenbelt, Maryland. Lauren.Schlenker@nasa.gov

<sup>†</sup> Aerospace Engineer, Navigation and Mission Design Branch. NASA Goddard Space Flight Center, Greenbelt, Maryland. Nathan.K.Esantsi@nasa.gov

<sup>‡</sup> Senior Navigation Engineer, Navigation and Mission Design Branch. NASA Goddard Space Flight Center, Greenbelt, Maryland. Joel.J.K.Parker@nasa.gov

the existing and well-proven GNSS architecture around the Earth during development of future lunar-centric architectures and to augment those architectures once established.

In-flight demonstrations of cislunar GNSS are needed to prove feasibility and to lay the groundwork for future development of cislunar GNSS technology. Past missions such as NASA’s Magnetic Multiscale (MMS) mission, which uses the NASA Navigator receiver to meet orbit determination accuracy requirements, have shown that GPS signals can be acquired as high as 29 Earth Radii (RE), providing concrete evidence suggesting the possibility of signal acquisition as far as the Moon.<sup>6</sup> However, the ability to extend GNSS-based navigation further from the Earth and to the Moon must be proven in flight before additional efforts can focus on developing operational equipment for future lunar missions.

The LuGRE payload was selected as one of ten NASA payloads to be flown onboard the Commercial Lunar Payload Services (CLPS) program Task Order 19D flight, awarded to Firefly Aerospace, Inc. for development and launch. The Firefly Blue Ghost Mission 1 lander will deliver the LuGRE payload to the Mare Crisium basin on the near side of the Moon, arriving in 2024 and operating for a minimum of 12 Earth-days on the surface of the Moon.

In the short time since the CLPS selection in 2021, extensive analysis has been performed by the LuGRE team, composed of members from the NASA Goddard Space Flight Center (GSFC), the Italian Space Agency (ASI) and the GNSS receiver manufacturer Qascom S.r.l., to characterize system properties and predict expected performance.<sup>7</sup> The aim of many of these analyses has been to inform inter-organizational discussions and design decisions that ensure maximum benefit to the LuGRE science investigations. LuGRE is just one of the many disparate payloads onboard BGM1, so it is critical to precisely understand the baseline mission needs required to satisfy science and engineering goals. This paper will describe key analyses of expected payload performance that have been performed to enable a successful implementation of the LuGRE mission onboard BGM1.

## LUGRE MISSION

The LuGRE mission aims to satisfy 3 key objectives towards the overall goal of demonstrating GNSS-based lunar PNT. In support of each of these objectives, 23 primary investigations have been identified as top priorities that shall drive design choices, with 10 being labeled as high-priority; Table 1 summarizes each top-level mission objective with corresponding high-priority science investigations.

**Table 1: LuGRE Mission Objectives and Driving Science Investigations**

<b>Objective #1:</b> Receive GNSS signals at the Moon. Return data and characterize the lunar GNSS signal environment.
Measure the signal strength throughout the mission and empirically evaluate link budget model.
Determine signal availability throughout the mission.
Measure Doppler-shift and Doppler-rate profiles throughout the mission.
Measure pseudorange from visible satellites during all planned operations periods.
<b>Objective #2:</b> Demonstrate navigation and time estimation using GNSS data collected at the Moon.
Calculate and characterize least-squares multi-GNSS point solutions throughout the mission where sufficient signals are available.
Calculate and characterize Kalman filter based navigation solutions onboard throughout the mission.

Compare onboard navigation solutions to external sources (e.g., ground-based measurement processing, planned trajectory, Blue Ghost navigation solution).
Characterize position, velocity, and time uncertainty and convergence properties throughout mission.
<b>Objective #3:</b> Utilize collected data to support development of GNSS receivers specific to lunar use.
Process GNSS observables (e.g., Doppler, pseudorange) with ground-based tools to predict achievable onboard navigation performance.
Calibrate ground models with LuGRE data and utilize to predict achievable navigation performance for future missions.

### Concept of Operations

The LuGRE payload will acquire and track GPS L1 and L5 signals and Galileo E1 and E5a signals, producing pseudorange, Doppler, and carrier phase measurements. These measurements will be used onboard to perform real-time navigation, as well as be downlinked to the ground for more in-depth ground-based navigation experiments. These measurements and resulting navigation data will be collected in transit from the Earth to the Moon, in lunar orbit, and on the surface of the Moon. Additionally, short spans of raw L1/L5 I/Q baseband samples will be collected so that raw samples may be replayed into ground-based receivers to inform future receiver development.

The LuGRE concept of operations within the BGM1 flight is shown in Figure 1.

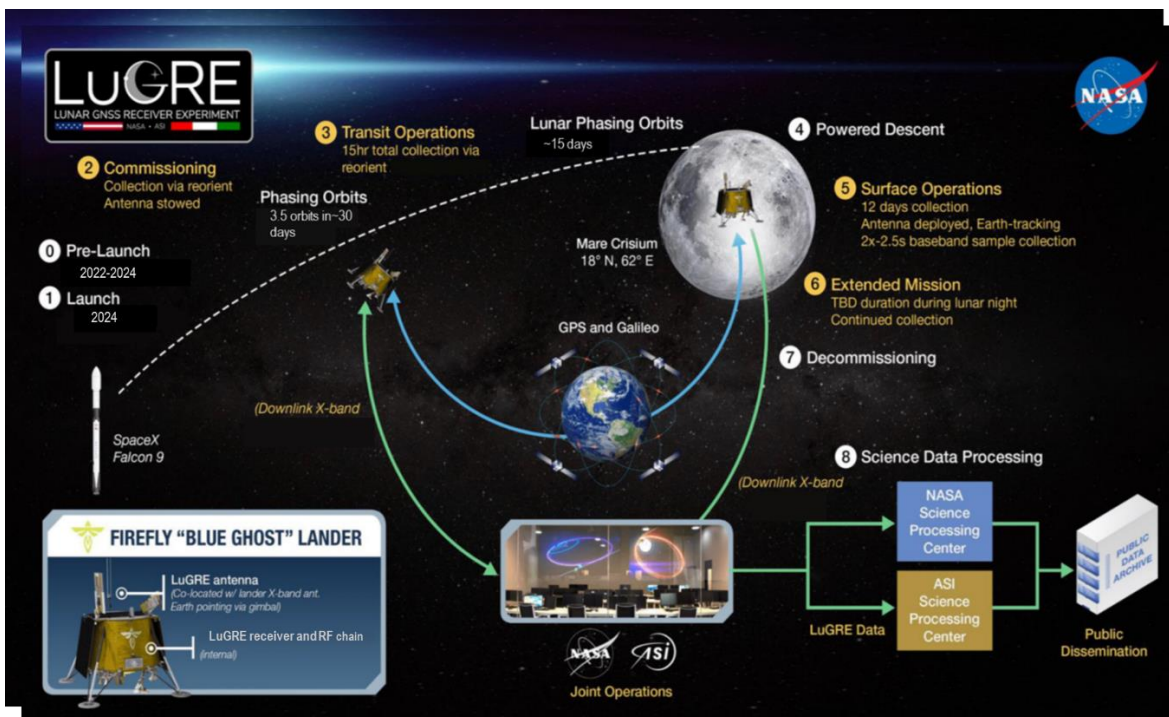


**Figure 1: LuGRE Concept of Operations**

BGM1 is slated for launch in 2024 from Cape Canaveral. A Falcon 9 launch vehicle will place the lander into a series of 3.5 phasing loops. Each phasing loop has a period of ~8.5 days, with apogee altitude near 55 RE and perigee altitude ranging from 1,000 to 4,000 km. After the phasing loops, the first Lunar Orbit Insertion (LOI1) maneuver will establish a highly eccentric lunar-centered orbit; LOI2 will lower perigee, and finally LOI3 will circularize the lander into a 100km

altitude lunar orbit where the lander will remain for approximately 14 days prior to powered descent to the surface.

Once safely on the lunar surface LuGRE will collect and downlink science data to the Earth, operating nearly continuously for 12 days, minus approximately 48 hours around lunar noon where the payload may be duty-cycled in one-hour increments to conserve power. An extended mission during lunar night is possible; if attempted, LuGRE is expected to continue to operate until power is lost and the payload is decommissioned.

To bridge the altitude gap in data between the GPS signals obtained by MMS at ~30RE altitude and the signals to be obtained on the surface (~60 RE), LuGRE will also collect GNSS data in transit, both during the phasing loops and in lunar orbit. This will provide a more complete picture of the GNSS signal environment in cislunar space as a function of altitude, which is the dominant factor affecting signal strength and ultimately availability of GNSS signals.

The duration of data collection time during transit is restricted due to the LuGRE high gain antenna being stowed during transit, as the entire lander must be reoriented to point the antenna towards the Earth for signal reception. The lander uses cold-gas thrusters for attitude control, and the availability of helium places a limit on the number of reorientation slews and total holding time possible to support LuGRE data collection. In total, the LuGRE mission is limited to up to 15 hours of total pointing time during transit operations, with a baseline of 1 hour of continuous pointing per discrete operation.

Given the time restriction on data collection during transit, Figure 2 shows the resulting planned schedule of payload operations for LuGRE, depicted in both distance from the Earth in units of Earth Radii (RE) and in lunar altitude once inserted into lunar orbit. Yellow circles represent the location of maneuvers; deterministic maneuvers (AIM, LOI 1-3, DOI) are specifically pointed out, while others represent opportunities for course correction if needed. Brown dots represent a baseline set of 15 planned 1-hour periods where LuGRE will be oriented to the Earth for data collection. This schedule represents the minimum planned operational duration during transit, though with available margin more may be possible. This baseline schedule of operation periods was selected by attempting to obtain a diversity of collection altitudes, while also utilizing opportunities for pre- and post- maneuver navigation analysis surrounding critical maneuvers, with the goal of comparing to ground-station tracking data collected at the same time as a LuGRE operation.

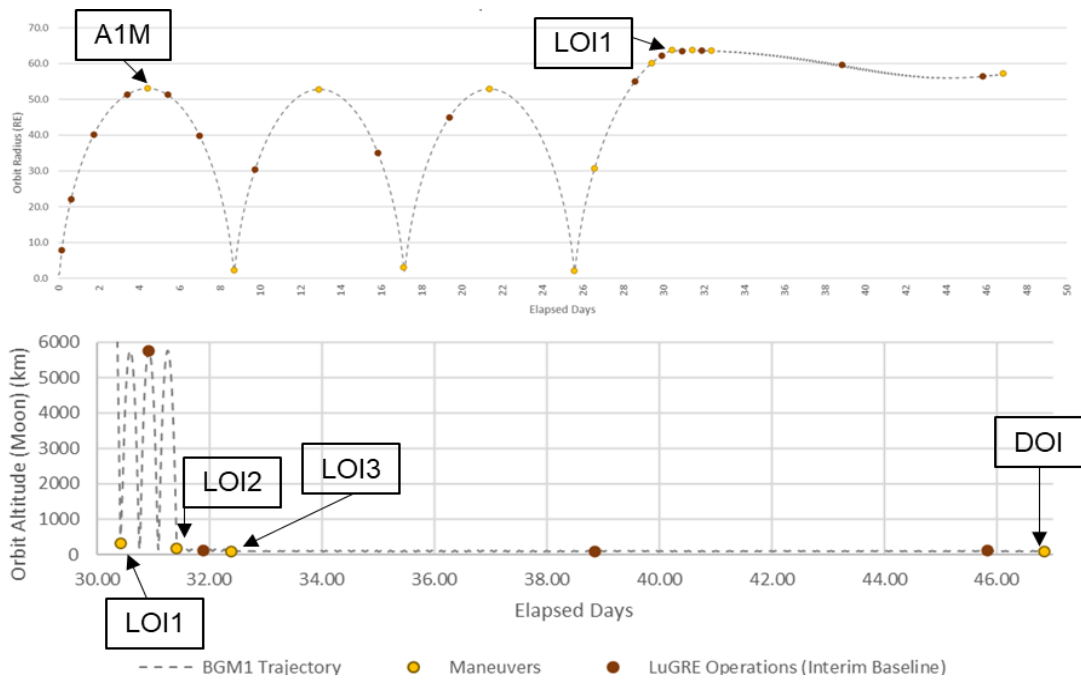


**Figure 2: LuGRE Operations Schedule During Transit**

### Receiver Design

The LuGRE receiver is designed for collecting and processing cislunar GPS and Galileo L1/E1 and L5/E5a signals as weak as 20 dB-Hz using high performance tracking, processing, and navigation algorithms. The receiver is developed by Qascom S.r.l. based on the QN400 model with suborbital and LEO Cubesat heritage.<sup>8</sup> The system contains two redundant receiver boards in a cold-redundant configuration. The operational receiver can be selected in-flight by a supervisory board either autonomously or manually via telecommand. The RF chain consists of a low noise amplifier, filter, and a high gain antenna with a measured peak boresight gain of ~16 dB at the L1 frequency; the receive antenna pattern for the high gain antenna manufactured by Haigh-Farr is shown in Figure 3. In total, the LuGRE payload consisting of the receiver, high gain antenna, low noise amplifier, and harnessing requires  $\leq 14$  W of power and  $< 5$ kg of mass.

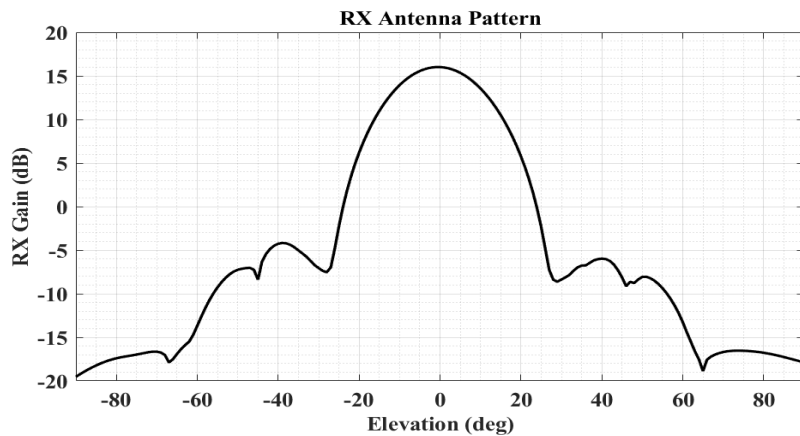


**Figure 3: Expected 1-D receive antenna pattern for the LuGRE antenna in the L1 band.**

Of note for the navigation performance analyses in this paper, the LuGRE receiver uses a GNSS-grade Voltage Controlled Temperature Compensated Crystal Oscillator (VCTCXO) for frequency discipline on the receiver board. Compared to previous cislunar GNSS studies, which have often used relatively high-stability clocks for PNT such as a Rubidium Atomic Frequency Standard (RAFS) or an Ultra Stable Oscillator (USO), it is expected that the VCTCXO will provide less stable timing accuracy.<sup>9</sup> However the choice of a lower-quality oscillator is a trade worth investigating, as this choice represents a lower SWaP-C option that may be more feasible for future small missions. Where relevant, the results in this paper investigate and quantify the effect the lower quality clock may have on navigation performance so that flight data collected by LuGRE can be used to predict performance that may be obtained using higher quality clocks.

Given the relatively large distances at which LuGRE will be acquiring GNSS signals, biases in onboard clock knowledge will have a subsequently larger impact on navigation performance and must be well characterized and accurately modeled. Figure 4 depicts the clock stability properties modeled for the LuGRE receiver in terms of Allan deviation, following the methodology of previous lunar GNSS studies.<sup>9</sup> This model is assumed to be representative of a typical space-grade VCTCXO – actual stability of the specific flight-model oscillator will be measured pre-flight and used to more accurately model expected performance during operations. In contrast with clocks used on past studies<sup>9</sup>, while the modeled VCTCXO at  $\tau = 100$ s has an Allan deviation on the order of  $1 \times 10^{-9}$ , a model for an USO has an Allan deviation on the order of  $1 \times 10^{-12}$  while the highest stability RAFS model has an Allan deviation on the order of  $2 \times 10^{-13}$ , therefore impacts to navigation performance as a result of clock stability are expected and must be understood.

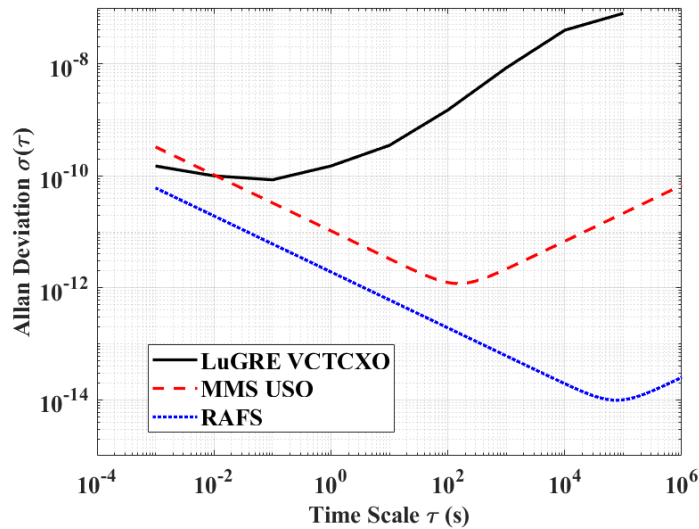


**Figure 4: Predicted conservative VCTCXO clock stability used for modeling, compared to other clock models used for previous analyses.**

## SIMULATION SETUP

The LuGRE receiver software has an onboard navigation module that will produce navigation solutions in real time, both from an Extended Kalman Filter (EKF) and through batch-least squares estimation when  $\geq 4$  GNSS satellites are visible. For analysis shown in this paper, the Goddard Enhanced Onboard Navigation System (GEONS) Ground MATLAB Simulation (GGMS) tool is used to simulate GPS and Galileo signal visibility at the L1/E1 frequency and perform navigation in a manner that is similar to the navigation being performed onboard in real-time. GGMS is a

MATLAB front-end to GEONS, a GSFC-developed navigation filter with extensive flight heritage, and previously used to perform similar GNSS-based navigation analysis for MMS.<sup>6,10</sup> An ephemeris of the planned BGM1 trajectory is used as the truth trajectory to generate GPS and Galileo pseudorange and Doppler measurements, which are processed in the GEONS EKF.

The GGMS simulation uses the following link budget equation to model the C/N0 obtained by the receiver:

$$C/N_0 = P_T + G_T(\phi, \theta) - 20 \log\left(\frac{4\pi d}{\lambda_{L1}}\right) + G_R(\phi, \theta) - L_{pol} - 10 \log(kT_{sys}) - R_{loss}$$

where  $d$  is the line-of-sight distance of the receiver to the transmitting GNSS satellite,  $\lambda_{L1}$  is the L1/E1 carrier frequency,  $k$  is the Boltzmann constant, and the remaining implementation-specific parameters are summarized in Table 2. Although it is expected that the LuGRE receiver will acquire and track signals as low as 20 dB-HZ, an acquisition threshold of C/N0 > 23 dB-Hz is generally assumed in order to keep 3dB of margin for worst-case polarization losses and potential increases in system noise temperature due to environmental effects. The effect of this additional margin on signal visibility and resulting navigation performance is quantified throughout this paper.

**Table 2: Link Budget Parameters**

Receive-Side		Transmit-Side	
Parameter	Value	Parameter	Value
System Implementation Losses ( $R_{loss}$ )	0.9 dB	GPS Block IIR ( $P_T$ )	17.3 dBW
System Temperature ( $T_{sys}$ )	162 K	GPS Block IIR-M ( $P_T$ )	18.8 dBW
Polarization Losses ( $L_{pol}$ )	1 dB	GPS Block IIF ( $P_T$ )	16.2 dBW
Receive Antenna Gain ( $G_R(peak)$ )	16 dB	GPS Block III ( $P_T$ )	18.8 dBW
		Galileo ( $P_T + G_T(peak)$ )	11 dBW

The components of the LuGRE system have been designed to make possible acquisition of extremely weak GNSS signals by utilizing high gain components with low noise figures. Based on testing of the flight model hardware, system implementation losses ( $R_{loss}$ ) are expected to be under 1 dB, with a total system temperature  $T_{sys}$  of approximately 162 K under nominal environmental conditions. An average polarization loss  $L_{pol}$  of 1 dB is assumed, with the expectation that any increases in loss for this reason may be absorbed by the 3 dB or margin being considered for the link budget. Finally, the receiver antenna gain  $G_R(\phi, \theta)$  is modeled as shown in Figure 3 using post-environmental anechoic chamber data for the flight model antenna.

Block-specific transmitter powers  $P_T$  shown in Table 2 are obtained using calibrated analysis of high-altitude flight data captured by MMS<sup>9</sup> as well as on-orbit antenna pattern data collected from the GPS Antenna Characterization Experiment (ACE).<sup>11</sup> In the absence of publicly available transmit power data for Block III vehicles, values are assumed the same as those used for Block IIR-M. For Galileo transmitters, an 11dB total EIRP out to 20° off-boresight is assumed, as used in prior analysis by ESA for the Proba-3 mission.<sup>12</sup> Transmit antenna gain patterns are specified

per-vehicle as a function  $G_T(\phi, \theta)$  of off-boresight angle  $\phi$  and azimuth angle  $\theta$ , from a combination of the GPS ACE dataset for sidelobe gain and publicly available GPS IIR/IIR-M gain patterns for the main lobe.<sup>13</sup> The peak EIRP for each transmitter is thus the sum of the block-specific transmit power and the vehicle-specific antenna pattern. These modeling decisions represent the current best knowledge available for each term in the link budget corresponding to the transit-side of the link, and further calibration of uncertain terms such as Galileo transmit power will become possible once LuGRE flight data is collected.

To properly predict navigation performance due to the specific architecture of the LuGRE receiver, GGMS computes pseudorange and Doppler measurement noise as a function of received C/N0, which is applied as Gaussian white noise. These models, based on the specifics of the internal receiver tracking loops as well as the noise introduced by the oscillator instability<sup>14</sup>, are shown in Figure 5. Note the constant offset in the Doppler noise model, representing the proportion of the total noise due to the oscillator instability. This demonstrates how the statistical Doppler measurement error, along with pseudorange bias, is another aspect of the navigation performance that is affected by the specifications of the onboard clock. For the LuGRE receiver, it is assumed that Doppler measurements are obtained through averaging the output of the phase lock loop carrier phase measurements.

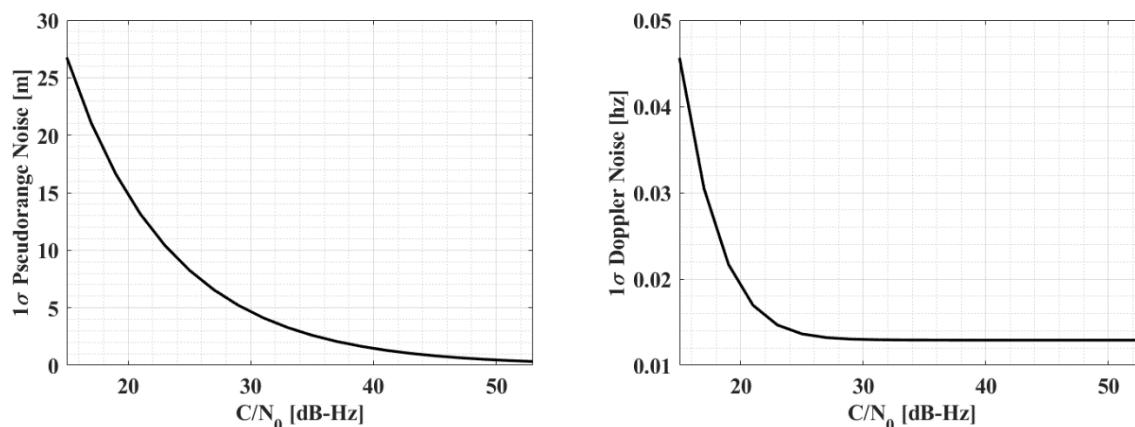


**Figure 5: Applied pseudorange and Doppler measurement noise as a function of signal strength.**

Although the LuGRE receiver will be producing and using carrier phase measurements in the onboard filter, future work remains to characterize the additional impact on navigation performance that carrier phase can offer as an observable.

### Predicted Signal Strength and Visibility

At cislunar distances where the angular separation of the GNSS transmitters leads to relatively poor dilution of precision (DOP) compared to what is standard for Earth-based observers, the number of signals available for processing becomes the largest predictor of navigation performance.<sup>15</sup>

Figure 6 illustrates the expected GPS-only, Galileo-only, and combined GPS/Galileo visibility throughout the LuGRE elliptical phasing orbits and low lunar orbits of the transit phase as a function of distance from the Earth. Visibility is defined as a satellite being geometrically in view (i.e. not occulted by either the Earth or Moon) as well as the acquired C/N0 for that satellite being above a specified threshold. In these figures, individual dots indicate the number of visible GNSS satellites over a single 5-minute period, while triangles represent the mean visibility over data collected



within altitude bins. The locations of the operational periods where flight data will be collected to verify these relationships are marked by vertical shaded bars.

These plots show that beyond the mean expected visibility, occasionally fewer or more satellites may be visible; for example, at 60 RE altitude 6 GNSS satellites are visible on average when using a 23 dB-Hz threshold, but that number may be as high as 9 at some instants of time or as low as 0 in others.

The left subplot shows the trend of visibility for an assumed nominal  $C/N_0$  threshold of 20 dB-Hz, while the right subplot shows the same trend for an assumed  $C/N_0$  threshold of 23 dB-Hz to account for possible losses; it is expected that the true visibility that will be seen in flight is somewhere between these two sets of data. The primary difference between the two thresholds is that a higher threshold removes on average of 1-2 satellites in general, with a much earlier drop-off in Galileo visibility when using a higher threshold (at 32 RE vs. at 52 RE, respectively) due to the conservatism of the Galileo EIRP pattern assumed. An additional benefit of LuGRE flight data at various altitudes will be the ability to confirm the uncertain Galileo transmit power based on when this drop-off is actually observed to occur.

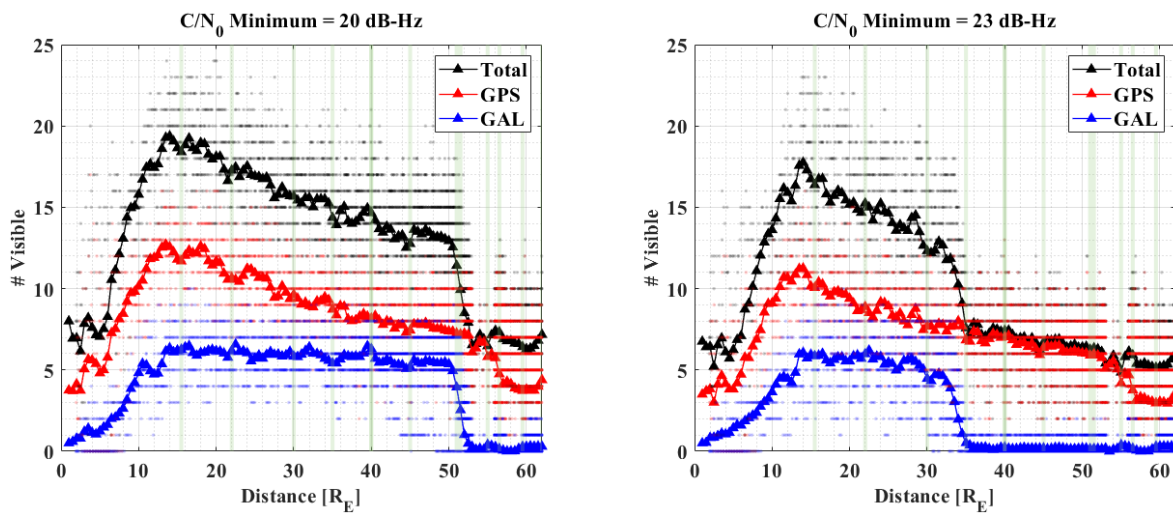


**Figure 6: Expected GNSS visibility characteristics throughout the transit phase of the LuGRE mission.**

Figure 7 shows similar information for the duration of the surface phase of the LuGRE mission, as a function of elapsed time on the surface, with triangles indicating mean visibility binned over 4-hour increments. While Galileo visibility is significantly lower than GPS, as expected due to the much lower peak EIRP, occasionally a single satellite may be seen.

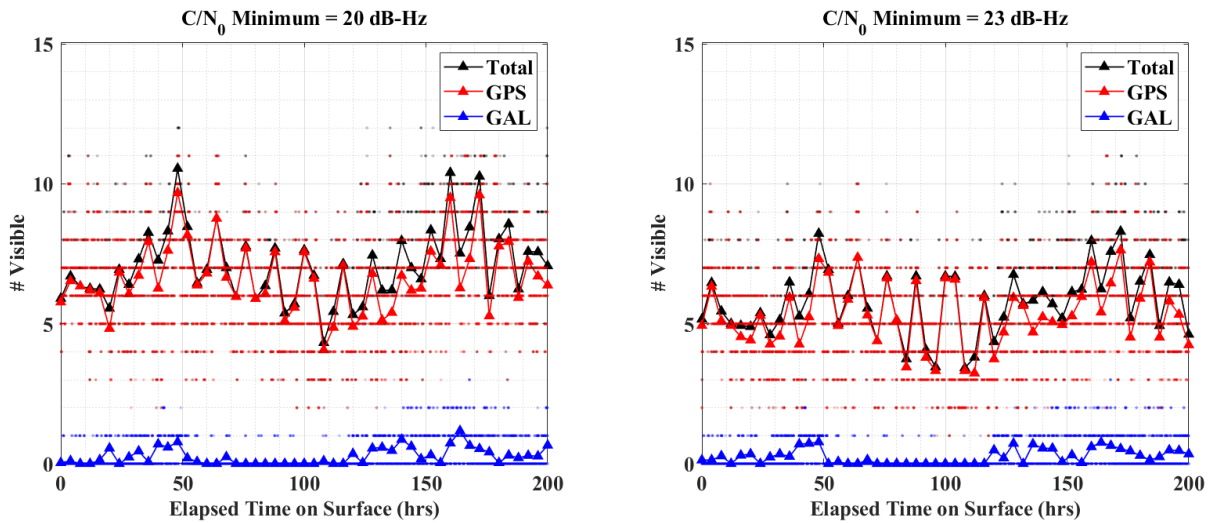


**Figure 7: Expected GNSS visibility characteristics throughout the surface phase of the LuGRE mission.**

These plots demonstrate the criticality of the defining elements of the LuGRE design when it comes to signal availability; just a few dB of received signal strength can make the difference between having a sufficient number of signals to navigate or not. Without the high gain design of the receive antenna, the relatively high-gain and low noise figure of the front-end amplifier, or the ability to acquire and track relatively low  $C/N_0$  signals, visibility would likely be too poor for navigation. Flight data proving these relationships are only available up to approximately 30 RE. Obtaining higher altitude data will be valuable for verifying these predictions and for driving lunar receiver decision decisions to maximize  $C/N_0$  tracking capability.

## ANALYSES

### Transit Operation Duration

Several unique aspects of LuGRE's status as one of several payloads onboard a CLPS mission raise questions that drive key systems engineering decisions made when planning the mission. One of these questions is how to best distribute the finite amount of observing time allocated to LuGRE. Given the challenge of being limited to 15 hours of total pointing time during the transit period of the mission, coupled with the desire to collect measurements at the greatest possible diversity of altitudes, a suite of analysis was performed to determine the minimum useful duration for a single operation period. The results of this analysis ultimately drove the creation of transit operations schedule shown in Figure 2; reaching this schedule required investigating of the key design aspects that determine how quickly the LuGRE receiver is expected to converge and obtain useful and interesting navigation data.

As shown in Figure 6, expected signal availability is low enough that EKF convergence is not expected to occur quickly. This is expected to be further exacerbated by the inherently poor DOP achievable at cislunar distances. Thus, EKF convergence rate and converged uncertainty is largely influenced by the measurement types used, as well as the quality of those measurements. While the GPS-based navigation solutions obtained using the MMS Navigator receiver at 29 RE represent the current highest use of GPS signals to-date, only GPS pseudorange measurements were used in the onboard GEONS EKF.<sup>6</sup> LuGRE will be able to utilize GNSS Doppler measurements so it is important to quantify the additional benefit to navigation performance that the availability of Doppler might have from the perspective of what is already known from flight data.

In typical GNSS use cases, the benefit to performance that GNSS Doppler measurements might contribute would be marginal; in the case of the LuGRE receiver however, GNSS pseudorange measurements are expected to have substantial bias due to the relatively high instability of the clock, especially at higher altitude as the distance the signals must travel is much larger. The presence of GNSS Doppler measurements grants an opportunity to provide additional information to balance out the clock-induced pseudorange noise and still obtain useful navigation solutions.

For these reasons, the following questions were posed for analysis to quantify how quickly the LuGRE EKF might achieve a level of meaningful convergence, and from this select a desired minimum operation duration:

- 1) Compared to flight data from the MMS mission, what is the expected additional benefit to using GNSS Doppler measurements in the EKF?
- 2) How much does the instability of the clock influence measurement noise and subsequent navigation filter convergence?
- 3) How much are these factors influenced by the 3 dB of margin imposed on the link budget?

Given the dramatic drop off in signal strength as a function of altitude, these questions were investigated at 3 altitudes:

- 1) 30 RE altitude
  - a. Aligning with similar flight data collected by MMS
- 2) 62 RE altitude
  - a. The highest altitude LuGRE will reach in transit prior to lunar orbit and the most challenging point of the transit from an observability standpoint at short time scales
- 3) Low Lunar Orbit (LLO)
  - a. Nearly-circular, 100km lunar altitude
- 4) Lunar surface
  - a. Stationary, at latitude 18°N, longitude 62°E

Each simulation is initialized with state error and uncertainty on the order of what may be expected from orbit determination and prediction obtained using traditional ground station tracking. Initial errors are randomly drawn from covariances with the following properties:

- 1) 30 RE altitude
  - a.  $1\sigma$ : 5 km position, 50 cm/s, 10 km clock bias, 300 m/s clock bias rate
- 2) 62 RE altitude
  - a.  $1\sigma$ : 5 km position, 50 cm/s, 10 km clock bias, 300 m/s clock bias rate
- 3) Low Lunar Orbit (LLO)
  - a.  $1\sigma$ : 10 km position, 100 cm/s, 10 km clock bias, 300 m/s clock bias rate
- 4) Lunar surface
  - a.  $1\sigma$ : 2.5 km position, 1 cm/s, 10 km clock bias, 300 m/s clock bias rate

GPS and Galileo pseudorange and Doppler measurements are simulated and ingested by the filter at a rate of 1 Hz for the orbital cases, and 1/30 Hz for the lunar surface case, with white noise applied as a function of C/N0 as shown in Figure 5. The 30 and 62 RE cases are run for 3 hours, while the LLO case is run for only 1.5 hours due to a 0.5-hour duration of signal occultation that occurs each orbit period as a result of nearly-polar orbital inclination.

Note that previous high-altitude GNSS results indicate that true formal convergence is likely not achievable without at least 1 full orbit of observation.<sup>6, 10</sup> This is incompatible with the limited operation duration available to LuGRE, making defining convergence in the traditional sense neither possible nor useful. Regardless, if the EKF is not diverging outright it remains instructive to

directly compare the properties of the achieved uncertainty for each situation in order to roughly quantify the impact of each. Metrics such as the relative differences rate of improvement and achieved accuracy are immediately clear from plots of the EKF covariance over the duration of a simulation.

Figure 8 through Figure 11 display the results of the listed trades and cases using the RSS position and velocity  $3\sigma$  uncertainty achieved throughout the duration of the simulation, with a vertical blue line indicating the 1-hour mark ultimately chosen as the maximum single operation length. For each figure, the influence of the assumed 3 dB margin on C/N0 is depicted with red lines for the 23 dB-Hz threshold, and black lines for the expected threshold of 20 dB-Hz. Additionally, the impact of processing Doppler as an observable alongside pseudorange is depicted with symbols; triangles represent pseudorange-only and stars represent the use of both pseudorange and Doppler observables. The top row of each figure represents results using the VCTCXO model used for LuGRE, while the bottom row represents the same trades using the MMS USO clock model.

*30 RE Case.* Figure 8 shows the navigation performance for an operation placed at an altitude of 30 RE. The bottom row “PR Only, 23 dB-Hz” curves show similar results as the orbit determination performance seen by MMS under similar conditions.<sup>6,10,15</sup> The top row of “PR+Dop, 20 dB-Hz” curves are most representative of what is expected for LuGRE at this altitude. In all cases, the addition of Doppler as an observable lends considerable improvement to performance. This improvement is particularly strong for results in the bottom row using the USO clock, due to the large portion of Doppler noise that is inherently attributed to clock stability. Therefore, when using a higher quality clock Doppler becomes an even more valuable measurement. Finally, the relative differences in performance between C/N0 thresholds indicate that reasonable accuracy can be achieved even with worst-case margin applied, but some improvement can be expected in the case that weaker signals can indeed be acquired.

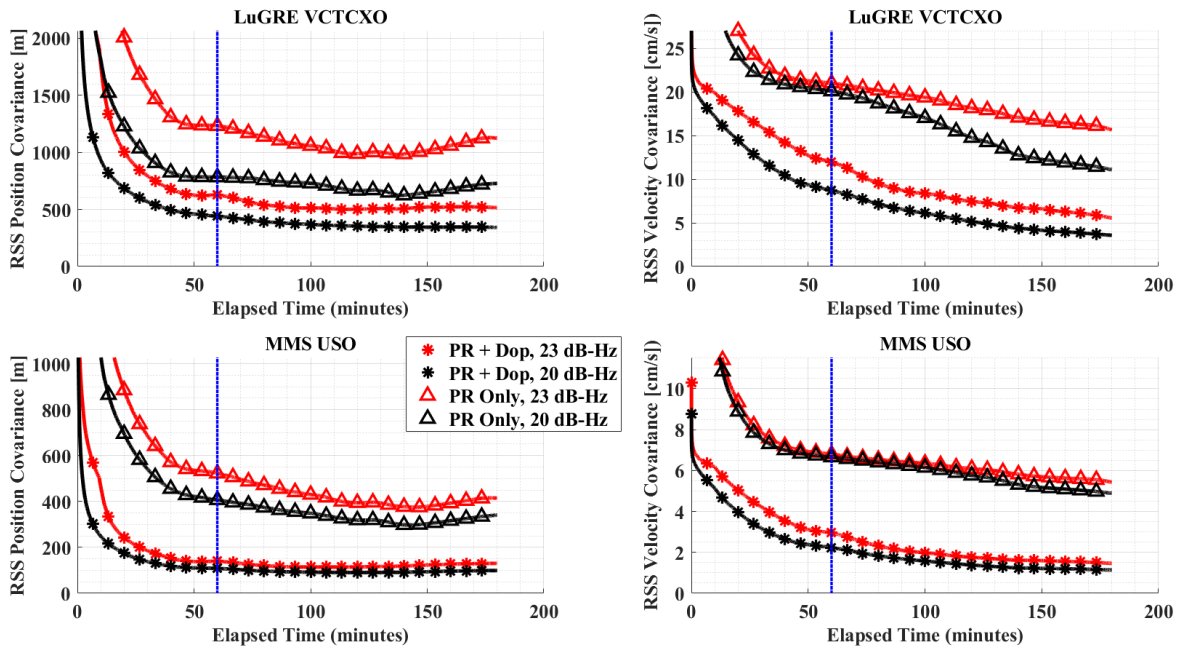


**Figure 8: Navigation performance at 30 RE.**

*62 RE Case.* Figure 9 shows the navigation performance for an operation placed at an altitude of 62 RE. The bottom row “PR Only, 23 dB-Hz” curves show what MMS may have seen at this

altitude, though this altitude was not actually realized in-flight. The top row of “PR+Dop, 20 dB-Hz” curves are most representative of what is expected for LuGRE if an operation period is placed at this altitude. This high-altitude case very near apogee of a highly elliptical orbit represents a challenge for observability as the dynamics are changing very slowly relative to short observation periods. For this reason, the addition of Doppler as an observable has a larger impact on performance, even more than the stability of the clock used. A larger impact to performance due to C/N0 margin is also seen, particularly in PR-only cases, further reinforcing that Doppler is an important capability in cases where very low C/N0 acquisition thresholds cannot be achieved.

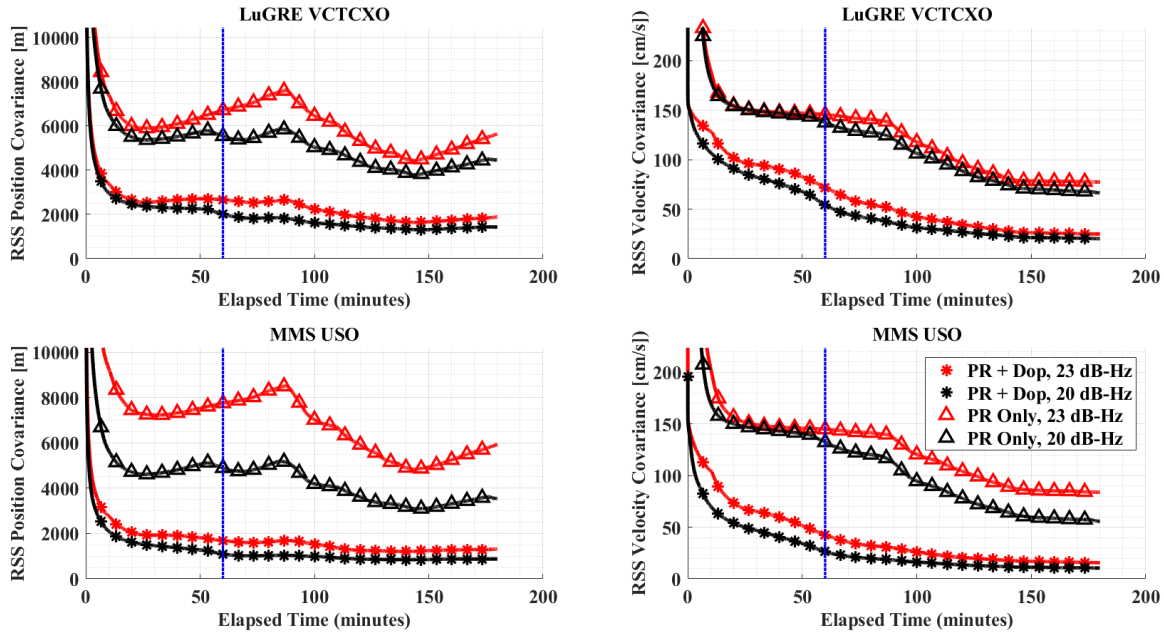


**Figure 9: Navigation performance at 62 RE.**

*Low Lunar Orbit Case.* Figure 10 shows the navigation performance for an operation placed in a nearly circular 100km altitude low-lunar orbit. Compared to the 62 RE case, a significantly larger percentage of the orbit period is covered on this time scale, leading to more robust convergence behavior overall. While the presence of Doppler as an observable continues to improve results considerably, the impact of a high stability clock is once again clear, allowing results to be more robust to changes in observability. Notably, changes due to satellite visibility are slight and only on the scale of minutes at a time as GNSS satellites pass in and out of view.

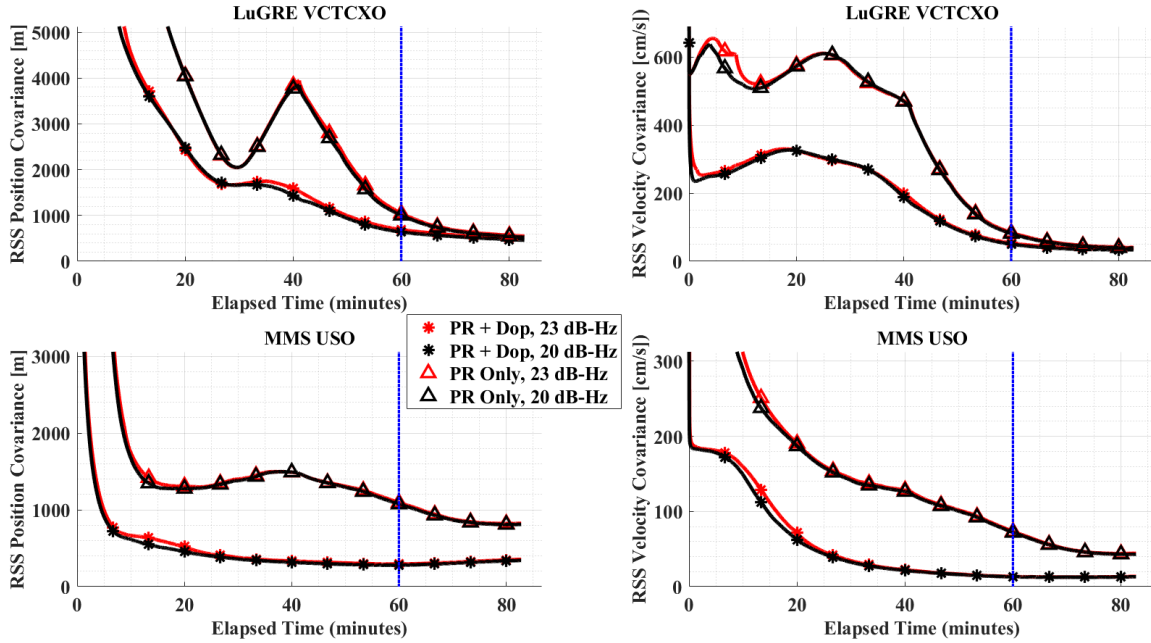


**Figure 10: Navigation performance for an LLO case using the LuGRE VCTCXO clock.**

*Surface Case.* Figure 11 shows the navigation performance for surface operations. Note that pointing time is not a constraint on LuGRE operations once the receiver is on the lunar surface, as cold gas propellant will not be required for pointing. Once the receiver is on the lunar surface, it will be continuously collecting data aside from a long outage during lunar night and occasional short outages for receiver reconfiguration. These results, while representing a stationary use case, continue similar trends as seen in previous cases; the addition of Doppler significantly aids convergence, more so than the stability of the clock used onboard. However, in the case of a lower quality clock, the difference in C/N0 threshold does appear to have a larger impact.

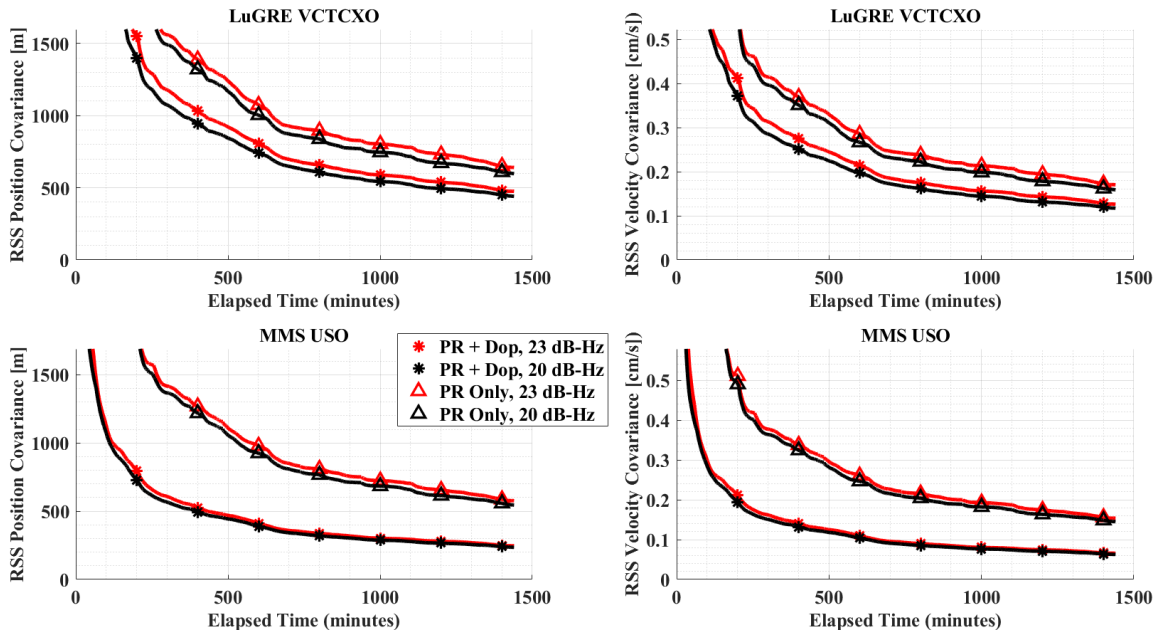


**Figure 11: Navigation performance for surface operations.**

From the sum of the LuGRE flight-representative information in these plots (i.e. using a 20 dB-Hz acquisition threshold and both pseudorange and Doppler measurements), the LuGRE team decided that a minimum operation duration of 1 hour should in general be planned. In future iterations of the operations schedule, a lower 30-minute navigation duration may be utilized in some cases to create additional time for I/Q sample collection while still maintaining adequate altitude diversity of collected data.

### Surface Science Data Volume

Once the Blue Ghost lander has landed on the lunar surface, LuGRE will have the opportunity to collect GNSS signals for the remaining duration of the mission, which lasts until the lander ultimately runs out of power and payloads are decommissioned. This final operational period may last as long as 12 days, with up to 5 days of continuous operation, and the option for an extended mission time days if the lander survives the harsh lunar night.

While the scientific benefit of this significantly longer duration data collection time is enormous, it presents additional challenge in the form of relatively large volumes of data that must be down-linked to the Earth. In contrast to LuGRE being generally the sole operational scientific payload when in transit, the surface operation period is the primary science period for the other 9 payloads onboard the lander. Consequently, data downlink bandwidth is a finite commodity that must be allocated wisely. Similar to the trades made in the Transit Operation Duration analysis section above, the question was raised of what measurement rate and data volume for LuGRE should be negotiated to obtain enough data to appropriately converge to a solution.

The LuGRE receiver hardware is limited to measurement rates of either 1 Hz or 1/30 Hz, and the baseline measurement downlink rate and volume is set to not exceed 4 kbps rate and 1.8 MB volume per hour. The performance of the filter is evaluated under these constraints to determine if these initial baseline requirements satisfy the data requirement for convergence and to inform the surface operation schedule. The EKF is initialized with the same state error and uncertainty in the Lunar surface case in the above Transit Operation Duration analysis section. Figure 12 and Figure 13 show the results of the trade using the RSS position and velocity  $3\sigma$  uncertainty determined in

the simulation, with the vertical blue line indicating when the 1.8 MB downlink volume threshold is met. For the downlink rate, the worst-case measurement message size is less than 4 kB, and the transmission rate is limited to 1 Hz or 1/30 Hz allowing the downlink rate limit is satisfy all cases.

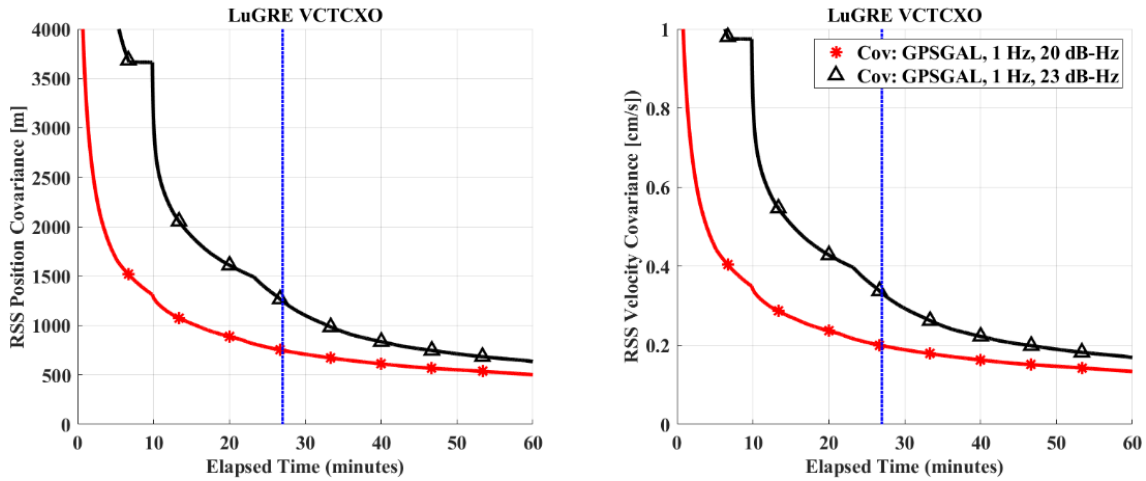


**Figure 12: Navigation performance for Surface case at a 1 Hz measurement rate**

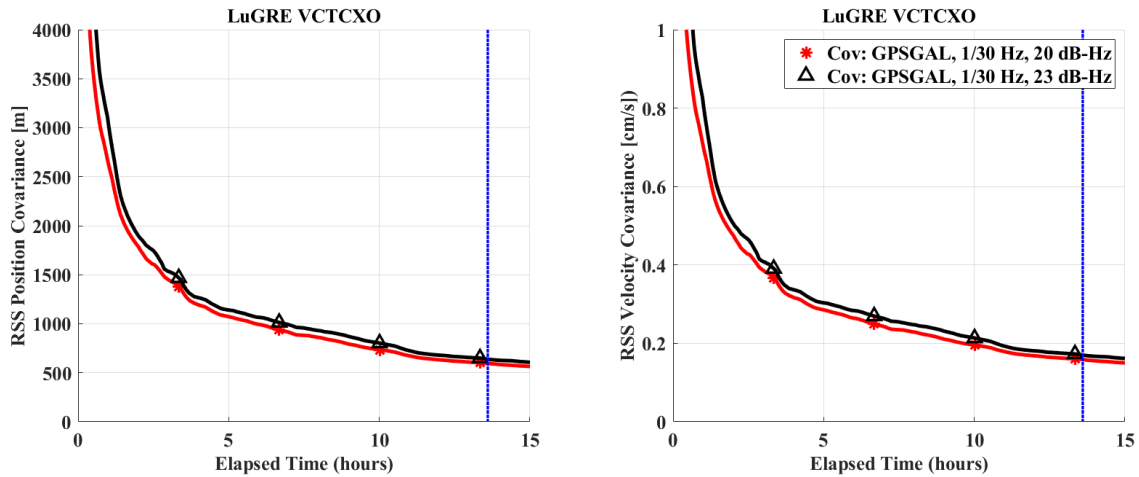


**Figure 13: Navigation performance for Surface case at a 1/30 Hz measurement rate**

Figure 12 shows that the receiver operating at a 1 Hz measurement rate exceeds the hourly downlink volume within 30 minutes, as indicated by the vertical blue line. The EKF converges quickly since the lander dynamics are that of a stationary body relative to the lunar surface and the primary driver of uncertainty being the pseudorange and Doppler measurements. However, given the constrained downlink bandwidth, operating at a 1 Hz measurement rate would require halting operations frequently and will provide a discontinuous picture of GNSS visibility from the surface. Using a 1/30 Hz measurement rate, shown in Figure 13, the downlink volume remains well under the downlink threshold, as indicated by the blue vertical line. A 1.8 MB downlink volume is not accumulated until 13.5 hours into the operational period.



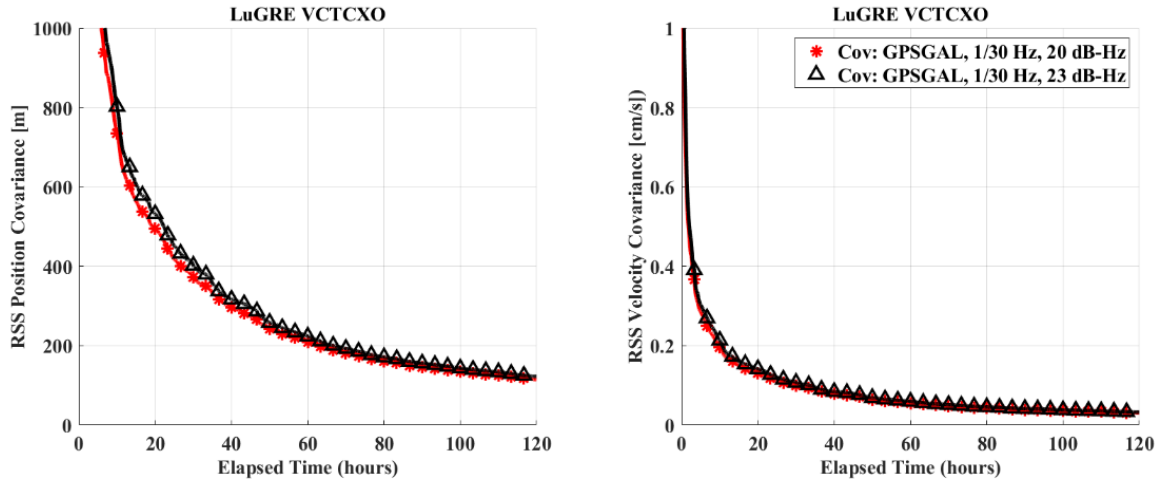


**Figure 14: Navigation performance for Surface case over an operational period**

With longer operational periods available on the surface, the performance of the LuGRE filter operating over a 5-day period, the longest available continuous period, at a 1/30 Hz measurement rate is shown in Figure 14. On these relatively longer time scales, the apparent difference in the convergence rate and accuracy for the 20 dB-Hz and 23 dB-Hz is minimal. In addition, the converged accuracy exceeds that of the 1 Hz rate in Figure 12 over the operational period.

## CONCLUSIONS

The Lunar GNSS Receiver Experiment mission, flying in 2024 onboard the Firefly Blue Ghost Mission 1 lander as part of the NASA Commercial Lander Payload Services program, aims to collect and navigate using GPS and Galileo signals in transit to, in orbit around, and on the surface of the moon. These signals will lend insight into the possibilities and challenges that must be overcome to realize GNSS as a feasible form of PNT in the broader lunar architecture. The details of the LuGRE mission implementation require careful modeling, planning, and analysis to ensure that the science that is returned within the scope of the mission constraints is both informative and useful to future receiver developers and mission planners.

The results of these analyses reveal interesting relationships on the key impacts to navigation performance at different points in a Moon-bound mission. It is apparent that the design choices that will enable LuGRE to obtain exceptionally weak GNSS sidelobe signals is critical to achieving the best performance possible, and any increases to system noise or losses in overall gain may quickly degrade the ability to navigate. Additionally, it is clear that the option to resolve Doppler as a GNSS observable is a significant driver to navigation performance in situations where observability is a challenge, as is the case for outbound trajectories from the Earth to the Moon. Finally, lunar orbit and surface results indicate that intentional design choice to prioritize these features can make GNSS-based PNT a feasible option towards enabling navigation technology for lunar landing.

## REFERENCES

1. Parker, J.J.K, et al., "The Lunar GNSS Receiver Experiment (LuGRE)." *International Technical Meeting*. Long Beach, CA: Institute of Navigation, 2022.
2. International Space Exploration Coordination Group, "Global Exploration Roadmap Supplement August 2020: Surface Exploration Scenario Update.", 2022. (Accessed 3 January 2022).

3. NASA, "2020 Artemis Plan." [https://www.nasa.gov/sites/default/files/atoms/files/artemis\\_plan-20200921.pdf](https://www.nasa.gov/sites/default/files/atoms/files/artemis_plan-20200921.pdf), 2020. (Accessed 3 January 2022).
4. Israel, D. "A LunaNet Implementation Approach." *Proceedings of the 16th International Conference on Space Operations*, SpaceOps 2021. 2021.
5. Schönfeldt, M., et al., "Across the Lunar Landscape Towards a Dedicated Lunar PNT System." *InsideGNSS*, November/December 2020.
6. Winternitz, L. B., Bamford, W. A., and Price, S. R. "New High-Altitude GPS Navigation Results from the Magnetospheric Multiscale Spacecraft and Simulations at Lunar Distances." *Proceedings of the 30th International Technical Meeting of the Satellite Division of The Institute of Navigation*. Portland, Oregon: ION GNSS+, 2017.
7. Parker, J. J. K., et al., "The Lunar GNSS Receiver Experiment (LuGRE)." *Proceedings of the 2022 International Technical Meeting of the Institute of Navigation*. Long Beach, CA: Institute of Navigation. 2022.
8. European Union Agency for the Space Programme, "Galileo is Heading to the International Space Station On Board The Cubesat Mission BOBCAT-1," October 2020, <https://www.euspa.europa.eu/newsroom/news/galileo-heading-international-space-station-board-cubesat-mission-bobcat-1> (Accessed 3 January 2022).
9. Winternitz, L. B., et al., "GPS Based Autonomous Navigation Study for the Lunar Gateway," *42nd Annual Guidance, Navigation, and Control Conference*. Breckenridge, CO: American Astronautical Society. 2019.
10. Winternitz, L. B., et al. "Global Positioning System Navigation Above 76,000 km for NASA's Magnetospheric Multiscale Mission." *NAVIGATION: Journal of the Institute of Navigation* 64.2. 2017.
11. Donaldson, Jennifer E., et al. "Characterization of On-Orbit GPS Transmit Antenna Patterns for Space Users." *NAVIGATION: Journal of the Institute of Navigation* 67.2. 2020.
12. Enderle, Werner, et al. "PROBA-3 Precise Orbit Determination based on GNSS observations." *Proceedings of the 32nd International Technical Meeting of the Satellite Division of The Institute of Navigation (ION GNSS+ 2019)*. 2019.
13. U.S. Coast Guard Navigation Center. "L Band Antenna Panel Patterns and Performance." <https://navcen.uscg.gov/lband-antenna-panel-patterns-and-performance>. Accessed June 2022.
14. Kaplan, Elliott D., and Christopher Hegarty. *Understanding GPS/GNSS: Principles and Applications*. Artech House, 2006. 2<sup>nd</sup> Ed.
15. Ashman, B.W. et al., "Application and Benefits of GNSS for Lunar Exploration." 16<sup>th</sup> International Conference on Space Operations. Virtual: International Astronautical Federation. 2021.